

Effect of a vertical guide plate on the wind loading of an inclined flat plate

Kung-Ming Chung^{*1}, Chin-Cheng Chou², Keh-Chin Chang² and Yi-Jun Chen²

¹*Aerospace Science and Technology Research Center, National Cheng Kung University, Taiwan*

²*Department of Aeronautics and Astronautics, National Cheng Kung University, Taiwan*

(Received September 14, 2012, Revised August 9, 2013, Accepted August 17, 2013)

Abstract. Wind tunnel experiments were performed to study the wind loads on an inclined flat plate with and without a guide plate. Highly turbulent flow, which corresponded to free-stream turbulence intensity on the flat roof of low-rise buildings, was produced by a turbulence generation grid at the inlet of the test section. The test model could represent a typical solar collector panel of a solar water heater. There are up-stream movements of the separation bubble and side-edge vortices, more intense fluctuating pressure and a higher bending moment in the turbulent flow. A guide plate would result in higher lift coefficient, particularly with an increased projected area ratio of a guide plate to an inclined flat plate. The value of lift coefficient is considerably lower with increased free-stream turbulent intensity.

Keywords: solar collector; inclined flat plate; turbulence intensity; guide plate; wind loads

1. Introduction

A flat plate normal to an air stream represents a common situation for wind loads on structures, such as noise barriers and signboards (Holmes 2001, Oaulotto *et al.* 2006). The flow is deflected around the plate, and the pressure distribution on the leeward wall is more uniform (resulting from slow-moving air in the wake) in comparison with that on the windward side. Moreover, there is more contribution of drag from the front face than from the rear face. Holmes (2007) indicated that the drag coefficient of a square wall with its plane normal to the flow is about 1.1. With a flat plate inclined to the flow, e.g., solar panels, the wind loads are dependent on tilt angle, wind direction and aspect ratio of the panel. For an inclined flat plate of infinite span in a free-stream, Fage and Johansen (1927) demonstrated that the drag and lift coefficients increased with tilt angle. The vortices generated at each edge passed downstream with a decreased frequency at a lower tilt angle.

The life cycle of the trailing edge vortex determined the structure and the size of the counter-rotating recirculation region leading to an asymmetric vortex sheet behind the inclined plate (Breuer and Jovicic 2001). A universal Strouhal number of 0.160 ± 0.003 was obtained by Chen and Fang (1996).

*Corresponding author, Professor, E-mail: kmchung@mail.ncku.edu.tw

Solar water heaters are mostly installed on the roof of low-rise buildings (10–15 m). Wind loads on ground-mounted solar arrays (or inclined flat plates) are less studied (Radu and Axinte 1989, Wood *et al.* 2001, Kopp *et al.* 2002). Chung *et al.* (2011) examined an inclined flat plate in smooth uniform flow. Stronger negative longitudinal differential mean pressure was observed, corresponding to strong wind loads. A guide plate at the leading edge of an inclined flat plate resulted in a decrease in wind uplift (Chung *et al.* 2011, 2013). Furthermore, field measurements of a strong typhoon at 13.5 m height by Cao *et al.* (2009) showed that free-stream turbulence intensity (TI) decreases with wind speed and remain almost constant when the wind speed becomes high, say $TI = 10\text{--}20\%$. It is well known that turbulence could enhance mixing and entrainment of free shear layer. For a blunt flat plate, Li and Melbourne (1995, 1999) showed the size of the separation bubble was reduced with increasing free-stream turbulence intensity. The main effect of large-scale turbulence was to reduce the magnitude of stream-wise pressure in the region near the leading edge. It was also found that fluctuating pressure increased from a minimum near separation to a maximum near the reattachment position. As the free-stream turbulence intensity increased, the location of peak fluctuating pressure moved closer to the leading edge. In this study, a turbulence generation grid was installed to investigate the effects of free-stream turbulence intensity on an inclined flat plate with and without a guide plate. Both mean and fluctuating pressures were measured. The lift coefficients on the upper and lower surface were evaluated by integrating the mean pressure distributions. Peak pressures on an inclined flat plate in smooth uniform and turbulent flows were also compared.

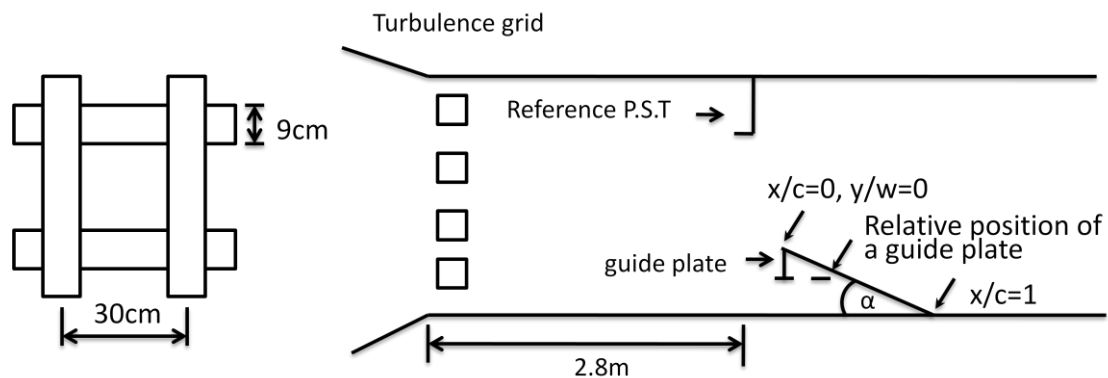


Fig. 1 Schematic drawing of wind tunnel, model, and turbulence generation grid

2. Experimental setup

2.1. Wind tunnel and test model

The experiments were conducted in the low speed wind tunnel of the Architecture and Building Research Institute. The facility comprises a honeycomb and three screens, and the contraction ratio is 4.71. The constant-area test section is 2.6 m tall, 4 m wide and 36.5 m long. A plan view and an elevation view of the working section are shown in Fig. 1. The free-stream velocity was measured by a pitot-static tube (PST), which was located at 2.8 m, 1.45 m and 0.8 m from the turbulence

generation grid, top wall and side wall of the tunnel, respectively. In this experiment, a turbulence generation grid (Roach 1986) was installed at the inlet of the test section. A grid of the square mesh type was adopted. The dimensions of the grid are 9-cm square wood and 30-cm mesh size. The leading edge of the test model was located at 2.8 m from the turbulence generation grid.

The baseline test model (G0 case, about 60% of a commercial solar collector) is an inclined flat plate, which is 120 cm (length) x 60 cm (width) x 5.5 cm (thickness). Also as shown in Fig. 1, the front edge of the inclined flat plate corresponds to $x/c = 0$, and y/w is the span-wise distance from the left-side edge, looking at the plate upwind. The plate was facing the flow direction at tilt angle α of 15° , 20° , 25° and 30° , in which the front edge is 31-60 cm from the tunnel floor. Note that the rear edge of the plate sat on the wind tunnel wall. The blockage ratio ranged from 1.55 to 4.5%, and no blockage corrections were applied to the present results. For the pressure model, it is considered that there are strong pressure gradients (flow separation and reattachment) near the leading edge of the plate. Therefore, 92% of pressure taps were machined on the first two-third of the plate, as shown in Fig. 2. Furthermore, two solid guide plates (70 cm wide and 0.5 cm thick) were fabricated. The height of each guide plate was 17.5 cm (G1 case) and 35 cm (G2 case), respectively. The guide plate also faced normal to the flow direction and was connected to the front edge of the inclined flat plate.

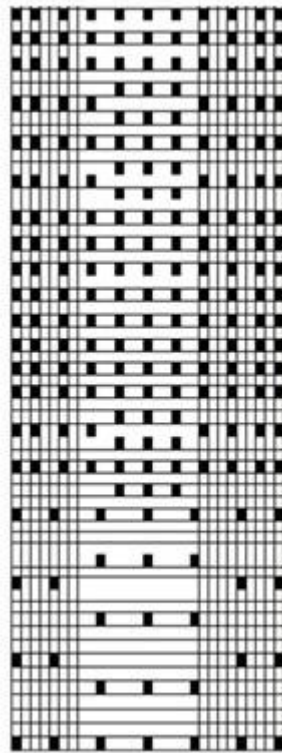


Fig. 2 Arrangement of pressure taps (solid symbols)

2.2. Measurement techniques

For the free-stream turbulence intensity ($= U_{rms}/U$) measurements, a hot-wire system composing an X-type hot wire (Dantec 55P61), a Dantec (Model 90N10) hot-wire anemometer (CTA, 90C10 module), an A/D converter (NI cDAQ-9178; Model 9215), and a light-duty 2-D traversing system were used. The frequency response of the hot-wire anemometer is 25 kHz as quoted by the manufacturer, and the sampling rate was 1 kHz. The traversing system was mounted at 2.8 m (about 9 times of the mesh size) from the inlet of the test section to support the hot-wire probe. In the absence of the turbulence generation grid, the free-stream turbulence intensity was about 0.3% (smooth uniform flow). When the turbulence generation grid was installed, the distributions of mean stream-wise velocity and turbulence intensity are shown in Fig. 3, in which $U = 12.1 \pm 1.6$ m/s and $TI = 11.4 \pm 1.2$ % (turbulent flow) at $Z^* < 0.25$, respectively. The appearance of overshoot velocity is observed, which agrees with the study by Owen and Zienkiewicz (1957). The velocity peak due to the accelerating action of the pressure drop across the grid on the fluid in the boundary layer suffers a smaller change in total pressure on passing through the grid than fluid in the main stream. Furthermore, the u-component of turbulence integral length scale was 12.3 cm, and the Reynolds number based on the length of the inclined flat plate Re_c was 8.77×10^5

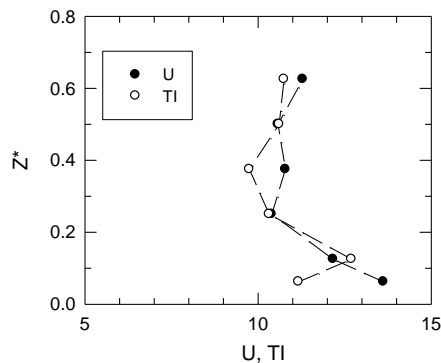


Fig. 3 Distributions of free-stream velocity (m/s) and turbulence intensity (%) (2.8 m from the inlet of the test section)

The surface pressure measurements were conducted with seven Scanivalve multichannel modules (Model ZOC 33/64Px 64-port, scan rate = 45 kHz), in which differential pressure transducers (Model RAD3200) were used. The full-scale range of sensors is $\pm 2,490$ Pa (or ± 10 inch H₂O), and the accuracy is $\pm 0.15\%$ of the full scale. For the pressure tubing system, Irwin *et al.* (1979) indicated small phase distortions for short tubes of length of order 60 cm, which is also consistent with the results obtained by use of restrictors. Therefore, the pressure modules were placed inside the model. Pressure tapings were connected to flexible polyvinyl chloride (pvc) tubing of 1.1-mm internal diameter and 30 cm long. The sampling rate was 256 Hz for all the test cases, and each record contained 40,960 data points. The mean surface pressure measured were non-dimensionalized by the values of free-stream static pressure p_∞ and dynamic pressure q of incoming flow, in which $C_p = (p - p_\infty)/q$. The fluctuating pressure coefficient C_{sp} is given as σ_p/q . Further, the upper-surface $C_{L,up}$ ($= L_{up}/qA$) and lower-surface $C_{L,low}$ ($= L_{low}/qA$) lift coefficients

were evaluated by the integration of the mean pressure distributions, followed by calculation of the lift coefficient ($C_L = C_{L,up} - C_{L,low}$).

3. Results and discussion

3.1 Surface flow pattern

Chung *et al.* (2011, 2013) had previously found the presence of boundary layer separation and side-edge vortices for the present test configuration in smooth uniform flow. In this study, the oil-flow visualization technique was employed to visualize the surface flow patterns. A thin film of mixture comprising titanium dioxide and silicon oil was applied on the upper and lower surface of the test models, for locating boundary layer separation, re-attachment, and side-edge vortices. Fig. 4 shows the oil flow pattern on the left-half upper surface at $\alpha = 15^\circ$ and $TI = 0.3\%$ for the G0 Case. Separated flow and side-edge vortices can all be observed on the plate surface. These phenomena occur because the shear layer from free-stream rolls toward the front-edge of the inclined flat plate and forms a large vortex. The side-edge vortices also impact the upper plate surface. It is considered that horseshoe vortex in counter-clockwise direction is formed due to the interactions of primary vortex near the front edge and side-edge vortices. Note that the horseshoe vortex on the right-half upper surface rotates in the opposite (clockwise) direction.

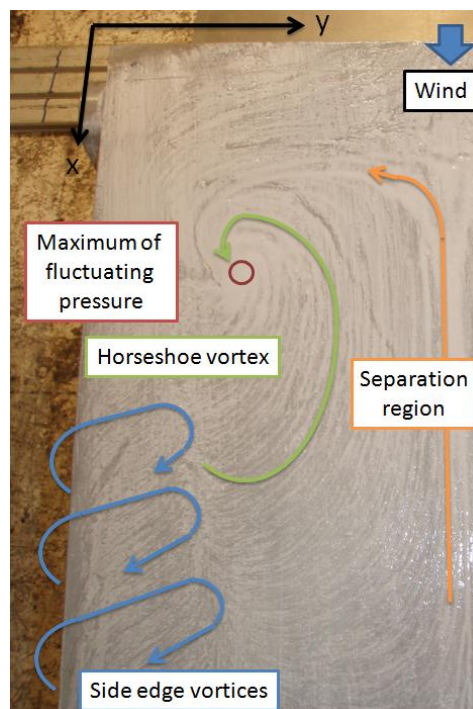


Fig. 4 Oil flow pattern on left-half upper surface $\alpha = 15^\circ$ and $TI = 0.3\%$ for G0 Case

The surface flow patterns can also be visualized by the contour plots of mean and fluctuating pressures. Fig. 5 shows the distribution of mean pressure coefficient C_p on the left-half upper surface for the G0 case at $\alpha = 15^\circ$. Note that C_p distribution is almost symmetrical with respect to the centerline of the inclined flat plate. In smooth uniform flow (TI = 0.3%), the vortices are observed near the front and side edges of the plate. With higher free-stream turbulence intensity (TI = 11.4%), the amplitude of C_p on the right-half upper surface decreases near the front edge. The reattachment location and side-edge vortices appear to move upstream, which agrees with the study by Li and Melbourne (1995). In other words, increased free-stream turbulence intensity tends to shorten the flow reattachment length for an inclined flat plate. Furthermore, the contour plots of fluctuating pressure coefficient C_{sp} are shown in Fig. 6. In smooth uniform flow, a higher level of C_{sp} is associated with the horseshoe vortices. Also note that increased free-stream turbulence intensity would enhance the interactions of separation bubble and side-edge vortices, thus inducing more intense fluctuating pressure in turbulent flow.

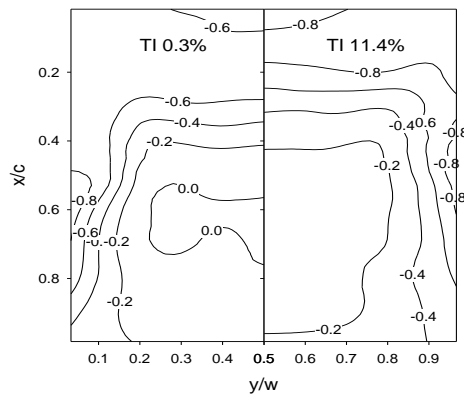


Fig. 5 Contour plots of mean pressure coefficient on upper surface, $\alpha = 15^\circ$, G0 case

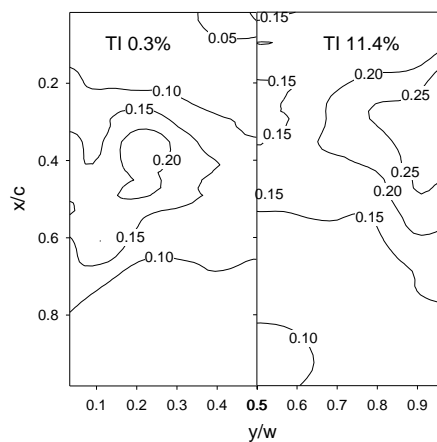


Fig. 6 Contour plots of fluctuating pressure coefficient on upper surface, $\alpha = 15^\circ$, G0 case

3.2 Longitudinal mean pressure distributions

Fig. 7 shows the C_p distributions along the centerline for the G0 cases, which can shed light on the effect of the free-stream turbulence intensity effects on aerodynamic characteristics of an inclined flat plate. At $\alpha = 15^\circ$, there is suction (flow separation) near the front edge, followed by recompression up to the middle of the inclined flat plate on the upper surface in smooth uniform flow. At locations further downstream, the C_p level shows only minor variation. It is also noted that the variation in positive mean surface pressure is not significant on the lower surface. In turbulent flow, stronger flow expansion (or higher peak pressure) is observed on the upper surface near the front edge, as shown in Fig. 7(a). This observation agrees with the finding of Hillier and Cherry (1981), in which the C_p level in the separation bubble is reduced with increased free-stream turbulence intensity. At the second half of the inclined flat plate, there is a slightly more negative pressure region. In addition, more positive pressure action can be seen on the lower surface, indicating higher wind loads with increased free-stream turbulence intensity. At a higher tilt angle ($\alpha = 30^\circ$), the flow development (expansion and recompression) follows a similar trend to that at $\alpha = 15^\circ$. However, the C_p levels are more negative on the upper surface and more positive on the lower surface up to $x/c \approx 0.4$, as shown in Fig. 7(b). In other words, the effect of tilt angle on the flowfield is only observed near the front edge and induces higher pressure difference. Regarding the effect of free-stream turbulence intensity, the C_p distributions near the front edge are roughly the same for both test cases. Only slightly more negative pressure action on the upper surface and slightly more positive pressure action on the lower surface are observed, resulting in a small increase in wind loads.

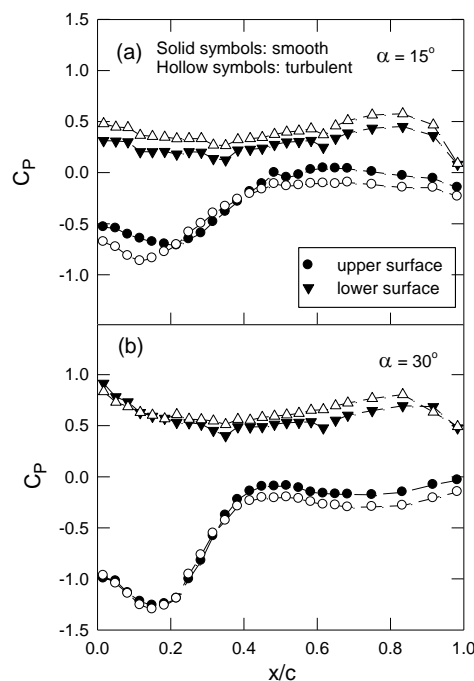


Fig. 7 C_p distributions along the centerline, G0 case

Furthermore, local wind loads in the longitudinal direction could be visualized from the distributions of differential mean pressure coefficient ($\Delta C_p = C_{p,up} - C_{p,low}$). The data in Fig. 7 are re-plotted and shown in Fig. 8. As can be seen, the ΔC_p level at $\alpha = 30^\circ$ is more negative in comparison with that at $\alpha = 15^\circ$, indicating greater uplift force with increasing tilt angle. For the effect of free-stream turbulence intensity, the distributions of ΔC_p at $\alpha = 30^\circ$ almost overlapped within the region at one-third distance from the front edge in either smooth uniform flow or turbulent flow. However, higher peak ΔC_p can be seen for the case at $\alpha = 15^\circ$ in turbulent flow, which corresponds to higher wind loads. Thus, it can be postulated that the effect of free-stream turbulence intensity on local wind loads becomes greater for a flat plate at a lower tilt angle.

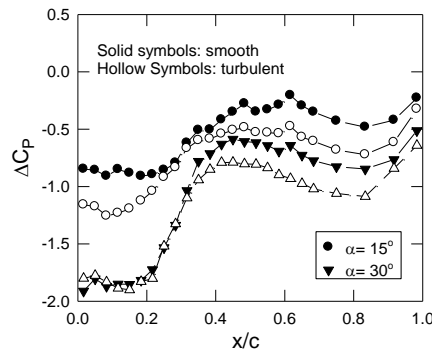


Fig. 8 ΔC_p distributions along the centerline, G0 case

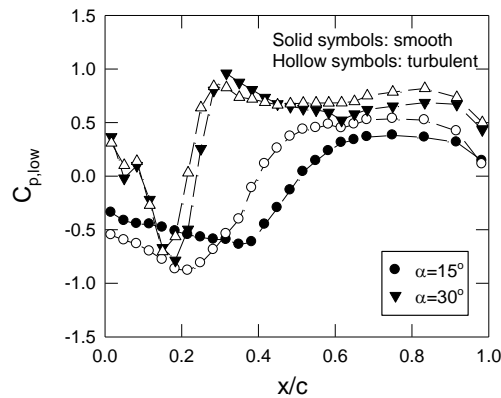


Fig. 9 $C_{p,low}$ distributions along the centerline, G1 case

For an inclined flat plate with a guide plate facing normal to the flow, Chung *et al.* (2013) found that the guide plate would affect both stream-wise and span-wise mean pressure distributions. Decreased C_p on the lower surface was observed, resulting in an increment in lift force of up to 62% in smooth uniform flow. In this study, a guide plate was also installed at the front edge of the inclined flat plate. Distributions of mean pressure coefficient on the lower surface with a shorter guide plate (G1 case) are shown in Fig. 9. The relative position of the tip of the guide

plate, as shown in Fig. 1, corresponds to $x/c = 0.563$ and 0.292 for $\alpha = 15^\circ$ and 30° , respectively. In turbulent flow, the peak pressure increases (more negative) and moves upstream from $x/c \approx 0.4$ to 0.2 for the $\alpha = 15^\circ$ case. The region of negative pressure action is narrowed down, and this might correspond to the change in the impingement location of the shear layer from the tip of a guide plate on the lower surface of the inclined flat plate. The wind loads at higher free-stream turbulence intensity would decrease near the front edge and increase at further downstream locations. At $\alpha = 30^\circ$, the free-stream turbulence intensity effect is less significant on $C_{p,low}$. This is similar to the G0 case, in which the distributions of $C_{p,low}$ are roughly the same in smooth uniform and turbulent flows.

3.3 Longitudinal fluctuating pressure distributions

Peak pressure is associated with surface pressure fluctuations and should be taken into account on peak design loads of an inclined flat plate. Fig. 10 shows distributions of the stream-wise fluctuating pressure coefficient on the upper surface $C_{\sigma p,up}$ at $\alpha = 15^\circ$ and 20° ($y/w = 0.5$) for the G0 case. It can be seen that peak pressure fluctuations are observed near the middle region of the inclined flat plate in smooth uniform flow. As mentioned above, higher $C_{\sigma p}$ level is considered to be associated with the horseshoe vortices (or interactions of separation bubble and side-edge vortices). It is also seen that the effect of tilt angle on the amplitude of $C_{\sigma p,up}$ is minimized near the front and rear edges. In turbulent flow, the level of $C_{\sigma p,up}$ is considerably higher than that in smooth uniform flow, except the case of $\alpha = 20^\circ$ at the middle region. In particular, peak pressure fluctuations are observed closer to the front edge at $\alpha = 15^\circ$. This observation is attributed to upstream movement of the separation bubble and side-edge vortices, as shown in Figs. 4 and 5. At $x/c = 0.3-0.5$, the amplitude of $C_{\sigma p,up}$ at $\alpha = 20^\circ$ is only slightly larger than that at $\alpha = 15^\circ$. The tilt angle effect is minimized at further down-stream locations.

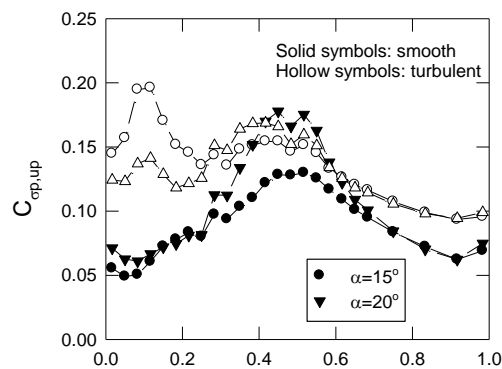


Fig. 10 $C_{\sigma p,up}$ distributions along the centerline, $y/w = 0.5$, G0 case

Fig. 11 shows distributions of surface pressure fluctuations on the lower surface $C_{\sigma p,low}$ ($y/w = 0.5$) for G0 cases. As can be seen, lower level of $C_{\sigma p,low}$ is observed at all tilt angles in smooth uniform flow. However, the ground effect would result in an increased $C_{\sigma p,low}$ near the rear edge. In turbulent flow, there is an increase in $C_{\sigma p,low}$. It is also noted that there is a peak $C_{\sigma p,low}$ near the front edge for the test case of $\alpha = 15^\circ$, which might be due to the intermittency of separated shear

layers (Saathoff and Melbourne 1999). For the effect of tilt angle, the amplitude of $C_{\sigma_p,low}$ decreases slightly near the front edge, and increases closer to the rear edge with higher tilt angle.

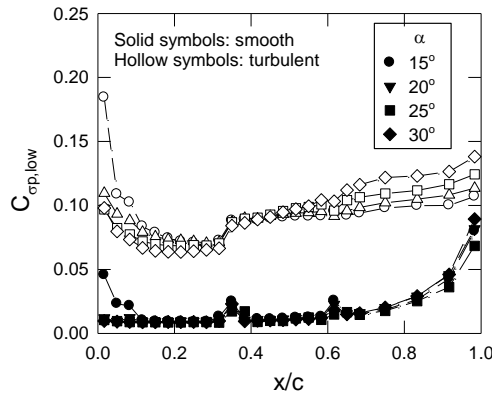


Fig. 11 $C_{\sigma_p,low}$ distribution along the centerline, $y/w = 0.5$, G0 case

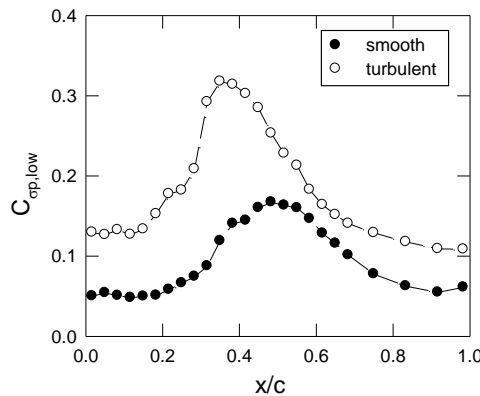


Fig. 12 $C_{\sigma_p,low}$ distributions along the centerline at $\alpha = 15^\circ$, $y/w = 0.5$, G1 case

Fig. 12 shows $C_{\sigma_p,low}$ distributions on the inclined flat plate with a shorter guide plate (G1 case). As mentioned above, the relative position of the tip of the guide plate corresponds to $x/c = 0.563$ for $\alpha = 15^\circ$. The $C_{\sigma_p,low}$ distribution shows a similar trend to that of G0 case. Increased free-stream turbulence intensity would result in higher $C_{\sigma_p,low}$. Peak pressure fluctuations are observed at further upstream locations in turbulent flow, which is consistent with the mean pressure distribution as shown in Fig. 9. It is also noted the $C_{\sigma_p,low}$ level for the G1 case is considerably higher than that of the G0 case within the projected area of the guide plate on the inclined flat plate. The peak $C_{\sigma_p,low}$ would correspond to the impingement of shear layer from the tip of the guide plate.

3.4 Spanwise pressure distributions

The mean span-wise pressure distributions C_{ps} could be used as an indicator of three-dimensional effect or side-edge vortices (Chung *et al.* 2008, 2011). Fig. 13 shows the distributions of $C_{ps,up}$ in smooth uniform and turbulent flows at $\alpha = 20^\circ$. The typical inverted U-shaped distributions at $x/c = 0.25$, 0.417 and 0.5 can be observed. Higher $C_{ps,up}$ occur near the centerline and the magnitude decreases when approaching the side edges. It is also seen that the distribution of $C_{ps,up}$ near the front edge, say $x/c = 0.25$, is more flattened, indicating the increased strength of side-edge vortices at $x/c = 0.5$. Furthermore, the suction action at $x/c = 0.25$ increases in turbulent flow when approaching side edges. However, there is less variation of $C_{ps,up}$ distribution at $x/c = 0.5$ implying upstream movement of side-edge vortices with increased free-stream turbulence intensity.

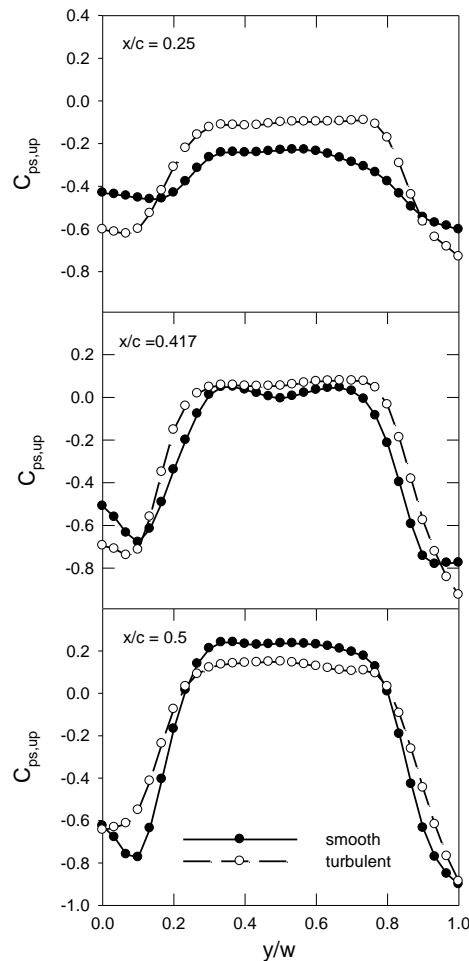


Fig. 13 $C_{ps,up}$ distributions at $\alpha = 20^\circ$, G0 case

The distributions of differential spanwise pressure coefficient (ΔC_{ps}) are also of interest. As shown in Fig. 14, all distributions show a similar W-shape for the G1 cases in both smooth uniform and turbulent flows. The negative pressure action near the side edges indicates that the lift force of an inclined flat plate might be mainly associated with the side-edge vortices. At $\alpha = 20^\circ$, the relative position of the tip of the guide plate corresponds to $x/c = 0.462$. The negative pressure action is more significant with increased free-stream turbulence intensity. When the flow is deflected over the guide plate and side edges, strong expansion would occur on the upper surface and result in lower lift force in turbulent flow. At $\alpha = 30^\circ$, stronger negative pressure action is also observed near the side edges in turbulent flow. However, the effect of free-stream turbulence intensity is less significant. Furthermore, higher negative pressure action near the side edges indicates an increased bending moment of an inclined flat plate in turbulent flow.

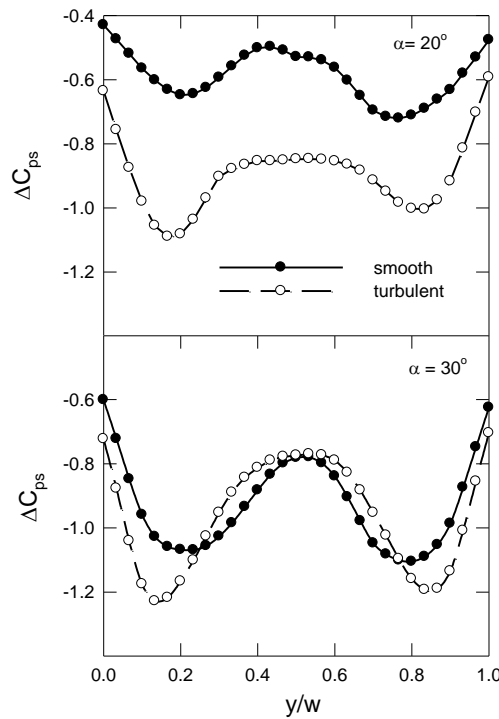


Fig. 14 ΔC_{PS} distribution at $x/c = 0.5$, G1 cases

3.5 Wind loads

Peak pressures $C_{p,peak}$ could be estimated at each pressure tap location from the time history of pressure signals. In this study, Peterka's method (1983) was adopted. In Fig. 15, it can be seen that the amplitude of peak pressure on the upper surface $C_{p,peak,up}$ decreases (higher suction pressure) with increasing tilt angle. The free-stream turbulence intensity effect is less significant for the G0 case. With a guide plate installed, there is a lower level of $C_{p,peak,up}$ in turbulent flow. On the lower surface, there is an increase in the amplitude of peak pressure $C_{p,peak,low}$ with the tilt angle for all

test cases in both smooth uniform and turbulent flows. An increase in free-stream turbulence intensity results in higher peak pressure.

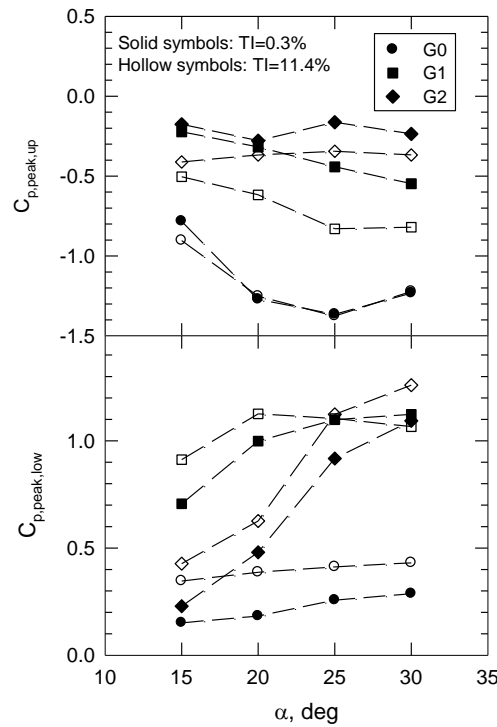


Fig. 15 Peak pressure coefficient on upper and lower surfaces

The lift coefficient on the upper and lower surfaces ($C_{L,up}$ and $C_{L,low}$) can be evaluated by integrating $C_{p,up}$ and $C_{p,low}$, respectively. In this study, the tilt angle and projected area ratio A^* (Chung *et al.* 2011, 2013) appear to be the dominant parameters on the lift force of an inclined flat plate. Thus, $C_{L,up}$ and $C_{L,low}$ for all test cases are plotted versus α/A^* , as shown in Figs. 16 and 17, respectively. On the upper surface, $C_{L,up}$ decreases linearly with α/A^* in both smooth uniform and turbulent flows. The effect of free-stream turbulence intensity would result in more negative $C_{L,up}$ (or larger negative lift force). On the lower surface, the data is slightly scatter and the effect of freestream turbulence intensity is less significant. However, the present data clearly show that $C_{L,low}$ increases with α/A^* and seems to approach some asymptotic values. More positive $C_{L,low}$ is associated with a smaller cavity formed between the guide plate and the inclined flat plate (smaller project area of a guide plate), and the increment in lift force is less significant. Furthermore, the lift coefficient C_L can be calculated from $C_{L,up}$ and $C_{L,low}$, as shown in Fig. 18. It is also seen that the effect of free-stream turbulence intensity on C_L is not significant at lower α/A^* , meaning that C_L difference in smooth uniform and turbulent flows would be reduced with a longer guide plate installed. With increasing α/A^* , the value of C_L in turbulent flow is considerably lower than that in smooth uniform flow.

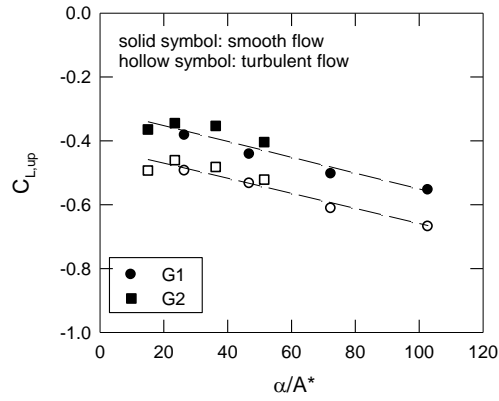


Fig. 16 Upper-surface lift coefficient

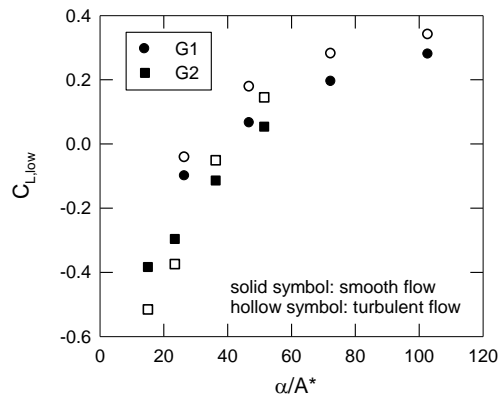


Fig. 17 Lower-surface lift coefficient

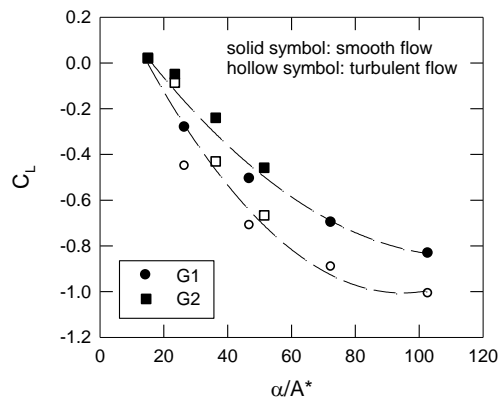


Fig. 18 Lift coefficient

4. Conclusions

Investigation on the effects of freestream turbulence intensity on the mean and fluctuating pressures of an inclined flat plate (or a solar collector panel) with and without a guide plate was performed. For the base-line model (without a guide plate), interactions of separation bubble and side-edge vortices would induce higher fluctuating pressure. With increased free-stream turbulence intensity, stronger flow expansion on the upper surface and more positive pressure action on the lower surface can be seen, which corresponds to higher wind loads. The increased tilt angle induces slightly higher pressure difference, which is observed only near the front edge. For an inclined flat plate with a guide plate, the peak pressure fluctuations correspond to the impingement of shear layer from the tip of a guide plate. As free-stream turbulence intensity increases, the flow is deflected inward. The peak pressure fluctuations are observed closer to the front edge. In the span-wise direction, the W-shaped distributions of differential pressure coefficient are observed. At lower tilt angle, increased free-stream turbulence intensity results in a higher bending moment in turbulent flow. The lift coefficient is associated with the tilt angle and projected area ratio of a guide plate and an inclined flat plate. A similarity parameter α/A^* is proposed to correlate all test conditions. The free-stream turbulence intensity effect is not significant at lower α/A^* . With increasing α/A^* , the value of C_L in turbulent flow is considerably lower than that in smooth uniform flow.

Acknowledgements

This work was under the support by the Bureau of Energy, Ministry of Economic Affairs, Taiwan, Republic of China.

References

- Breuer, M. and Jovicic N. (2001), "Separated flow around a flat plate at high incidence: an LES investigation", *J. Turbul.*, **2**, 1-15.
- Cao, S., Tamura, Y. Kikuchi, N., Saito, M. Nakayama, I. and Matsuzaki, Y. (2009), "Wind characteristics of a strong typhoon", *J. Wind Eng. Ind. Aerod.*, **97**(1), 11-21.
- Chen, J.M. and Fang Y.C. (1996), "Strouhal number of inclined flat plates", *J. Wind Eng. Ind. Aerod.*, **61**(2-3), 99-112.
- Chung, K.M., Chang, K.C. and Liu, Y.M. (2008), "Reduction of wind load on a solar collector model", *J. Wind Eng. Ind. Aerod.*, **96**(8-9), 1294-1306.
- Chung, K.M., Chang, K.C. and Chou, J.C. (2011), "Wind loads on residential and large-scale solar collector models", *J. Wind Eng. Ind. Aerod.*, **99**(1), 59-64.
- Chung, K.M., Chang, K.C., Chen, J.K. and Chou, C.C. (2013), "Guide plate on wind uplift of a solar collector", *Wind Struct.*, **16** (2), 213-224.
- Fage A. and Johansen F.C. (1927), "On the flow of air behind an inclined flat plate of infinite span", *P. Roy. Soc. London - A*, **116** (773), 170-197.
- Hillier, R. and Cherry, N.J. (1981), "The effects of stream turbulence on separation bubbles", *J. Wind Eng. Ind. Aerod.*, **8**(1-2), 49-58.
- Holmes, J.D. (2001), "Wind loading of parallel free-standing walls on bridges, cliffs, embankments and ridges", *J. Wind Eng. Ind. Aerod.*, **89**(14-15), 1397-1407.
- Holmes, J.D. (2007), *Wind loading of structures*, 2nd Ed, Taylor & Francis, London and New York.

- Irwin, H.P.A.H., Cooper, K.R. and Girard, R. (1979), "Correction of distortion effects caused by tubing systems in measurements of fluctuating pressures", *J. Wind Eng. Ind. Aerod.*, **5**(1-2), 93-107.
- Kopp, G.A., Surry, D. and Chen, K. (2002), "Wind loads on a solar array", *Wind Struct.*, **5**(5), 393-406.
- Li, Q.S. and Melbourne, W.H. (1995), "An experimental investigation of the effects of free-stream turbulence on stream wise surface pressures in separated and reattaching flows", *J. Wind Eng. Ind. Aerod.*, **54-55**, 313-323.
- Li, Q.S. and Melbourne, W.H. (1999), "The effect of large-scale turbulence on pressure fluctuations in separated and reattaching flows", *J. Wind Eng. Ind. Aerod.*, **83**, 159-169.
- Oaulotto, C., Ciampoli, M. and Augusti, G. (2006), "Wind tunnel evaluation of mean wind pressure on a frame-type signboard", *J. Wind Eng. Ind. Aerod.*, **94**(5), 397-413.
- Owen, P.R. and Zienkiewicz, H.K. (1957), "The production of uniform shear flow in a wind tunnel", *J. Fluid Mech.*, **2**(6), 521-531.
- Peterka, J.A. (1983), "Selection of local peak pressure coefficients for wind tunnel studies of buildings", *J. Wind Eng. Ind. Aerod.*, **13**, 477-488.
- Radu, A. and Axinte, E. (1989), "Wind forces on structures supporting solar collectors", *J. Wind Eng. Ind. Aerod.*, **32**(1-2), 93-100.
- Roach, P.E. (1986), "The generation of nearly isotropic turbulence by means of grids", *Int. J. Heat Fluid Fl.*, **8**(2), 82-92.
- Saathoff, P. and Melbourne W.H. (1999), "Effects of freestream turbulence on streamwise pressure measured on a square-section cylinder", *J. Wind Eng. Ind. Aerod.*, **79**, 61-78.
- Wood, G.S., Denoon, R.O. and Kwok, K.C.S. (2001), "Wind loads on industrial solar panel arrays and supporting roof structure", *Wind Struct.*, **4**(6), 481-494.